International Journal of Nanomedicine

Dovepress
open access to scientific and medical research

Open Access Full Text Article

ORIGINAL RESEARCH

Ebselen Optimized the Therapeutic Effects of Silver Nanoparticles for Periodontal Treatment

Ye Liang[1–4,*], Bing Wang[1–4,*], Qing Yu[1–4], Weijia Wang[1–4], Shaohua Ge[1–4], Jinlong Shao[1–4]

[1]Department of Periodontology, School and Hospital of Stomatology, Cheeloo College of Medicine, Shandong University, Jinan, 250012, People's Republic of China; [2]Shandong Key Laboratory of Oral Tissue Regeneration, School of Stomatology, Shandong University, Jinan, 250012, People's Republic of China; [3]Shandong Engineering Research Center of Dental Materials and Oral Tissue Regeneration, School of Stomatology, Shandong University, Jinan, 250012, People's Republic of China; [4]Shandong Provincial Clinical Research Center for Oral Diseases, School of Stomatology, Shandong University, Jinan, 250012, People's Republic of China

*These authors contributed equally to this work

Correspondence: Shaohua Ge; Jinlong Shao, Tel +86 531 88382123; +86 531 88382597, Fax +86 531 88382923, Email shaohuage@sdu.edu.cn; jinlong.shao@sdu.edu.cn

Objective: Silver nanoparticles (AgNPs) possess excellent antibacterial effects on periodontal pathogens, but their clinical application is limited mainly due to their cytotoxicity through inducing oxidative stress in human cells. Ebselen disrupts the reactive oxygen species (ROS) scavenging in bacteria and relieves oxidative stress in mammalian cells. This study aimed to assess the antibacterial and anti-inflammatory effects of AgNPs and ebselen as well as the protective effect of ebselen, to further provide the theoretical basis for their future application in periodontal treatment.

Methods: The antibacterial and anti-biofilm effects of the synthesized AgNPs combined with ebselen were assessed on *Porphyromonas gingivalis* (*P. gingivalis), Streptococcus gordonii* (*S. gordonii*), and *Fusobacterium nucleatum* (*F. nucleatum*) in planktonic condition and as biofilms. In addition, the intracellular bactericidal efficiency of AgNPs and ebselen was evaluated in *P. gingivalis*-infected human gingival fibroblasts (HGFs). The cytotoxicity, intracellular ROS levels, and potential antioxidative enzymes were detected in HGFs treated with AgNPs and ebselen. Further, the anti-inflammatory effects were evaluated by in vitro and in vivo experiments.

Results: The combination of AgNPs and ebselen showed excellent antibacterial effects against planktonic *P. gingivalis* and *F. nucleatum* and synergistic antibiofilm effects on all mono- and multi-species biofilms. In addition, ebselen significantly enhanced the intracellular bactericidal efficiency of AgNPs. Furthermore, ebselen combined with up to 20 μg/mL AgNPs showed no obvious cytotoxicity to HGFs. Evidently, ebselen alleviated the AgNPs-induced ROS by increasing the levels of glutathione and superoxide dismutase 2. Moreover, AgNPs and ebselen together declined the release of *P. gingivalis*-stimulated inflammatory cytokines both in vitro and in vivo, and reduced alveolar bone resorption effectively.

Conclusion: AgNPs combined with ebselen would be an effective adjuvant for periodontal treatment owing to their synergistic antibacterial and anti-inflammatory effects.

Keywords: periodontitis, antibacterial, oxidative stress, anti-inflammation

Introduction

Periodontitis is a complex infectious disease initiated by bacteria, manifesting as pathologic loss of periodontal ligament and alveolar bone.[1] *Streptococcus gordonii* (*S. gordonii*) is an early colonizer that can easily attach to the tooth surfaces and facilitate the colonization of other periodontal pathogens to establish subgingival biofilms.[2,3] *Fusobacterium nucleatum* (*F. nucleatum*) can act as a bridge pathogen between the early and late colonizers by creating favorable conditions for the outgrowth of the late colonizer, such as *Porphyromonas gingivalis* (*P. gingivalis*), which is a keystone pathogen in the etiology of chronic periodontitis.[4] *P. gingivalis* can invade cells and tissues where they can maintain viability to avoid immune surveillance, thus easily developing antibiotic resistance and producing persistent infection.[5–7]

Received: 9 August 2023
Accepted: 14 December 2023
Published: 29 December 2023

Graphical Abstract

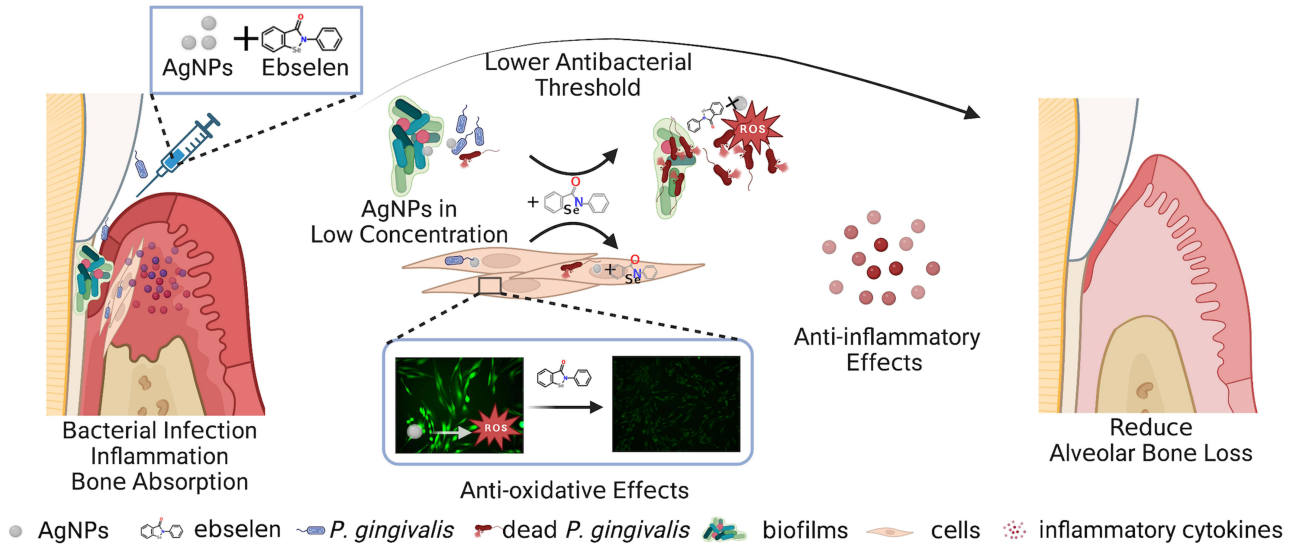

Therefore, the exploration of antibacterial agents against pathogens both planktonic grown and in biofilms or cells will facilitate periodontal treatment.

Silver nanoparticles (AgNPs) have been recognized as promising antibacterial agents that are efficient for both Gram-negative and Gram-positive bacteria.[8,9] They can kill bacteria by increasing membrane permeability and inducing reactive oxygen species (ROS) production through intracellular uptake.[8,9] Consequently, the therapeutic effects of AgNPs on dental caries or periodontal diseases are attributed to their antimicrobial efficacy against *Streptococcus mutans, Staphylococcus aureus* (*S. aureus*), and *P. gingivalis*.[9,10] As AgNPs can be phagocytized by cells, they exhibit high bactericidal efficacies against *S. aureus* in osteoblasts,[11] meanwhile, the autophagy induced by nanoparticles would also be beneficial for controlling intracellular *P. gingivalis*.[12] Moreover, AgNPs are reported with the capability to inhibit biofilm developing and destroy bacterial biofilms, which indicates they are potential agents combating bacteria protected by biofilms.[13,14] Nevertheless, their clinical application is still limited due to the concern over their toxicity. For instance, silver could be detected in organs after administration of massive AgNPs doses, especially in the liver and spleen,[8] and AgNPs-induced ROS increasing results in oxidative stress and cellular injury in human cells.[9,15] Hence, alleviating the intracellular oxidative stress and reducing therapeutic concentrations of AgNPs would facilitate their prospective application.

Intracellular oxidative stress is closely associated with the antioxidant systems in both bacteria and human cells. There are generally two thiol-dependent antioxidant systems, ie, thioredoxin (Trx) and glutathione (GSH) systems in most cells.[16] Both AgNPs and the released silver ions disturb the function of these two antioxidant systems by binding to thiol groups, and the disturbance is nonspecific to bacteria since it is also hazardous to human cells.[17,18] Coincidently, the structures of thioredoxin reductase (TrxR), a crucial enzyme in Trx systems, are different in bacteria and mammalian cells.[19] Ebselen can act as a TrxR inhibitor to disrupt ROS scavenging in bacteria,[20] while it serves as a substrate of TrxR and a mimic of glutathione peroxidase (GSH-Px) to relieve oxidative stress in mammalian cells.[21] Therefore, combining AgNPs with ebselen would be an optimized strategy to improve the antibacterial efficacy of AgNPs and reduce oxidative damage in mammalian cells. Accordingly, ebselen and AgNPs have been reported to possess synergistic antibacterial effects on both *S. aureus* and *Escherichia coli* (*E. coli*);[21] however, their antibacterial efficacy on periodontal pathogens of typical pathogenic status such as planktonic or in biofilms has yet been explored. Besides, the protective effect of

ebselen on AgNPs-induced oxidative stress and whether the combination could relieve bacteria-caused inflammatory reactions is still unknown.

Herein, we aimed to provide the theoretical basis for the future application of AgNPs and ebselen in periodontitis, by exploring the antibacterial effects of AgNPs and ebselen against periodontal pathogens in planktonic, biofilm, and intracellular status, as well as their effect on human gingival fibroblasts (HGFs) including the measurement of intracellular GSH content, TrxR activity, and superoxide dismutase (SOD)2 expression to further explore the protective effect of ebselen. Finally, the anti-inflammatory effects of AgNPs and ebselen both in vitro and in vivo were assessed by evaluating the expression of inflammatory cytokines such as interleukin (IL)-6, IL-8, C-C motif ligand 2 (CCL2), and their potential therapeutic effects on periodontal destruction were also evaluated by alveolar bone loss analysis in vivo.

Materials and Methods

Preparation and Characterization of AgNPs

AgNPs were synthesized by the classic Lee-Meisel method according to Yu's study.[22] Briefly, AgNPs as start seeds were synthesized by reducing from silver nitrate (Sigma, St Louis, MO, USA) with sodium borohydride (Sinopharm, Beijing, China) and trisodium citrate (Tianjin Damao Chemical, Tianjin, China). Then, AgNPs were further synthesized with the above seeds. To remove the residual agents, the synthesized AgNPs were washed twice with Milli-Q water. The concentration of AgNPs in the dispersant was determined by measuring dry weight. Then the ultraviolet-visible (UV-vis) spectrum of AgNPs was characterized by UV-vis spectrophotometer. The shape and particle size were also observed under transmission electron microscopy (TEM). The particle size, polymer dispersity index (PDI), and zeta potential were further measured by dynamic light scattering (DLS) analysis.

Evaluation of Antibacterial Effect Against Planktonic Periodontal Pathogens

P. gingivalis, F. nucleatum, and *S. gordonii* were obtained from the American Type Culture Collection (ATCC), and the types were ATCC 33277, ATCC 10953, and ATCC 10558, respectively. Firstly, the glycerol-cryopreservative bacteria were melted and spread on brain heart infusion (BHI, Qingdao Haibo, Qingdao, China) blood agar plates containing 1% agar powder, 5% defibrinated sheep blood, 5% hemin, and 0.5% vitamin K, to obtain pure colonies. The colony was then transferred into liquid BHI medium containing 5% hemin and 0.5% vitamin K (complete medium) and incubated in the anaerobic chamber (DG250, DWS, Winchester, England) with 80% N_2, 10% H_2, 10% CO_2 at 37°C for 24 to 48 h, and then the bacteria were used in the following experiments.

The bactericidal experiments were as follows: *P. gingivalis, F. nucleatum*, and *S. gordonii* in complete medium were added into the 96-well plate (50 μL/well) and treated with AgNPs (0, 5, 10 μg/mL in final concentration) and ebselen (0, 5, 10 μM in final concentration) for 24 h, and then the culture was diluted with a 10-fold gradient and 5 μL of each diluted suspensions were taken to drop onto the blood agar plates and incubated in anaerobic condition. Then the bactericidal efficiency was evaluated by colony-forming unit (CFU) counting method.

To evaluate the inhibitory effect of AgNPs and ebselen on the growth of *P. gingivalis, F. nucleatum*, and *S. gordonii*, bacteria in the complete medium were treated with various concentrations of AgNPs (0, 5, 10, 20 μg/mL in final concentration) and ebselen (0, 10 μM in final concentration), and then incubated in the anaerobic incubator, and the optical density (OD) of the culture suspensions at 600 nm were recorded at 24, 48, and 72 h by the microplate reader (BMG, Berlin, Germany), respectively.

Assessment of ROS Levels in *P. gingivalis*

1 mL of 5×10^7 CFU/mL *P. gingivalis* in complete medium containing AgNPs (0, 5 μg/mL in final concentration) and ebselen (0, 10 μM in final concentration) were incubated in anaerobic condition for 2 h, and then bacteria were collected by centrifuging and intracellular ROS was labeled by 2′,7′-dichlorofluorescein diacetate (DCFH-DA; Beyotime, Shanghai, China) according to the instruction of intracellular ROS assessment kit. The fluorescence images were

observed and taken by fluorescence microscope with a camera under 488 nm excitation, and mean fluorescence intensity was quantified by Image J.

Evaluation of Anti-Biofilm Effects

To analyze the inhibitory effect of AgNPs and ebselen on the biofilm formation of *P. gingivalis*, titanium sheets with a diameter of 14.75 mm were placed at the bottom of the 24-well plate, 500 μL of 1×10^8 CFU/mL *P. gingivalis* was added per well, and treated with different concentrations of AgNPs (0, 5, 10 μg/mL) alone or combined with 10 μM ebselen. The plate was placed in the anaerobic incubator for 48 h and then washed twice with sterilized phosphate-buffered saline (PBS), and 1 mL of 2.5% glutaraldehyde (Solarbio, Beijing, China) was added to each well for fixation at 4°C overnight. And then the samples were dehydrated with graded ethanol, freeze-dried, sprayed with gold, and taken for scanning electron microscopy (SEM, Hitachi, Tokyo, Japan) observation. Besides, the samples were also dyed with live-dead bacteria staining kit (Bestbio, Shanghai, China) to observe the viability of bacteria in the biofilms and the thickness of biofilms by confocal laser scanning microscope (CLSM, Andor, Purbeck, England). For the biofilm dispersion experiment, 500 μL of 1×10^8 CFU/mL *P. gingivalis* was inoculated on the titanium sheet in the 24-well plate for 24 h, washed twice, and then treated with AgNPs (0, 5, 10 μg/mL) or together with 10 μM ebselen in complete medium. The plate was placed in the anaerobic condition for another 24 h and the following steps were consistent with the biofilm formation experiment.

Moreover, *F. nucleatum* and *S. gordonii* biofilms were established using 1×10^8 CFU/mL and 1×10^6 CFU/mL bacterial suspension, respectively. The multispecies biofilm was established by mixing *P. gingivalis, F. nucleatum*, and *S. gordonii* in the ratio of 1:1:1 (10^8, 10^8, and 10^6 CFU/mL, respectively) and cultured anaerobically. The following process and detection methods were consistent with that of *P. gingivalis*. Moreover, the multispecies biofilms were also stained with crystal violet to evaluate the biomass.

Evaluation of Intracellular Bactericidal Efficiency

HGFs were obtained from gingival tissues removed in crown lengthening surgery and impacted teeth extraction surgery by enzyme digestion method as previously described.[23] Written approval for HGFs collection performed in this study was approved by the Medical Ethical Committee of Stomatological Hospital of Shandong University (Protocol No. 20211112) complying with the Declaration of Helsinki, and written informed consent was obtained from each individual participant.

HGFs were seeded in the 24-well plate at a density of 3×10^4 cells/well. After cell adhesion, HGFs were infected with *P. gingivalis* at a multiplicity of infection (MOI) of 100 for 2 h, and then washed with sterilized PBS thrice, 500 μL DMEM medium containing 500 μg/mL gentamycin was added for 30 min to eliminate extra bacteria, and then HGFs were treated with AgNPs (0, 5, 10 μg/mL) or combined with 10 μM ebselen for 4 h, after that, HGFs were washed three times, and 1 mL sterilized water was added into each well for 1 h to lyse HGFs, *P. gingivalis* inside HGFs were counted on the blood agar plates.

As to flow cytometry detection, *P. gingivalis* was labeled by 5(6)-Carboxyfluorescein diacetate N-succinimidyl ester (CFDA-SE; MKbio, Shanghai, China) according to the manufacturer's protocol. To only label the *P. gingivalis*, the *P. gingivalis* was pre-labeled with CFDA-SE. CFDA-SE can enter live bacteria and be catalyzed by the esterase into CFSE, and then CFSE is kept inside and binds with the amino on protein irreversibly. The residual CFDA-SE diffused into the medium and was removed by washing with fresh medium. The HGFs were infected with the pre-labeled *P. gingivalis* with fresh medium to avoid being labeled. The following procedure was consistent with the previously described. Finally, HGFs were collected for flow cytometry (BD, USA) to evaluate fluorescence intensity reflecting the amounts of intracellular bacteria.

Assessment of Cytotoxicity, Intracellular ROS Levels, and Antioxidative Enzymes in HGFs

HGFs were suspended in DMEM and seeded into the 96-well plate at a density of 3×10^3 cells/well. After cell adhesion, the cells were treated with AgNPs (0, 5, 10, 20 μg/mL) or together with 10 μM ebselen for 24 h, and the viabilities of HGFs were assessed by cell counting kit-8 (CCK-8, Dojindo, Kumamoto, Japan) as the instruction.

For detection of intracellular ROS levels, HGFs were inoculated into 6-well plates at a density of 2×10^5 cells/well. After cell adhesion, the cells were treated with AgNPs (0, 5, 10 μg/mL) or together with 10 μM ebselen for 6 and 24 h,

respectively. And intracellular ROS level was measured by fluorescent probe DCFH-DA according to the manufacturer's protocol. The fluorescence intensity was detected by flow cytometry. Besides, the ROS levels in HGFs at 24 h were also observed by fluorescence microscope (Leica, Wetzlar, Germany), and the mean fluorescence intensities were evaluated by image J.

To assess intracellular GSH amount, HGFs in the culture plate were treated with AgNPs (0, 5, 10 μg/mL) or together with 10 μM ebselen for 24 h, and then HGFs were collected and disrupted by quick freeze-thawing twice with liquid nitrogen and 37°C water. The supernatants were obtained for examination by GSH amount assay kit (Beyotime, Shanghai, China) with the instruction of the manufacturer's protocol.

To assess intracellular TrxR activity, HGFs in the culture plate were treated with AgNPs (0, 5 μg/mL) or together with 10 μM ebselen for 24 h, and then HGFs were collected and disrupted by ultrasonic lysis. The supernatants were obtained for examination by the TrxR activity assay kit (Solarbio, Beijing, China) according to the manufacturer's protocol.

HGFs in the culture plate were treated with AgNPs (0, 5, 10 μg/mL) or together with 10 μM ebselen for 24 h, and then RNA samples were collected by Trizol (Accurate biology, Beijing, China) for qRT-PCR examination to evaluate the expression of *SOD2*. The total RNA of cells was extracted according to the manufacturer's instructions using the Trizol reagent (Accurate biology, Beijing, China). The samples' messenger RNA (mRNA) concentrations were determined using the GeneQuant™ pro RNA/DNA Calculator Spectro photo meter (Amersham Biosciences, Pittsburgh, PA, USA). The ratio of absorption (OD 260 nm/OD 280 nm) was between 1.8 and 2.0. Then, RNA was converted to complementary DNA (cDNA) using a reverse transcriptase synthesis kit (Accurate biology, Beijing, China). qRT-PCR primers for *NADPH* and *SOD2* were listed in Table S1, qRT-PCR was performed in duplicate using Light Cycler 480 II Real-Time PCR System (Roche, Basel, Switzerland) with a two-step method. The PCR reaction system contained 5 μL of SYBR Green PCR mix (Accurate biology, Beijing, China), 0.2 μL of each primer, 1 μL of cDNA template, and 3.6 μL nuclease-free water in a final volume of 10 μL per reaction. The cycling parameters for qRT-PCR were 95°C for 30s, 45 cycles of 95°C for 5s, 60°C for 30s, and a melt curve assay was then performed (95°C for 5s, and then the temperature increased by 0.11°C every 1s) to detect the formation of primer-derived trimers and dimers. The real-time quantitative PCR reaction was performed in triplicate for each sample, and the mean value was used to calculate the mRNA expression levels. Expression levels of interested genes were normalized to *GAPDH*, by calculating the ΔCt (Ct gene of interest-average Ct housekeeping gene), and the expression of the interested gene was expressed as $2^{-(\Delta Ct)}$.

Evaluation of the Anti-Inflammatory Effect on HGFs Infected with *P. gingivalis*

HGFs were infected with *P. gingivalis* (MOI = 100) for 2 h and then treated with AgNPs (0, 5 μg/mL) or together with 10 μM ebselen for 24 h. The supernatants were collected to evaluate secretion of IL-6, IL-8, and CCL2 by enzyme-linked immunosorbent assay (ELISA; Biolegend, San Diego, CA, USA), and RNA samples were collected for qRT-PCR examination to evaluate the expression of *IL-6, IL-8, CCL2*, and *SOD2*. The total RNA extraction and qRT-PCR procedures were the same as above, and qRT-PCR primers for *NADPH, IL-6, IL-8, CCL2*, and *SOD2* were listed in Table S1.

Evaluation of Autophagic Flux in HGFs Infected with *P. gingivalis*

HGFs were seeded on glass coverslips in 24-well plates at the density of 3×10^4 cells/well. After cell adhesion, the cells were transfected with AdM-CMV-mCherry-EGFP-LC3B adenovirus (Vigene, Shandong, China) at MOI of 100 for 24 h. and the transfected cells were infected with *P. gingivalis* (MOI = 100) for 2 h, and then treated with AgNPs (0, 5 μg/mL) or together with 10 μM ebselen for 12 h. Cells were fixed for 15 min and then the coverslips were taken out for observation.

Experimental Periodontitis Establishment and in vivo Evaluation

Six- to eight-week-old male Wistar rats were provided by Beijing Vital River Laboratory Animal Technology Co., Ltd. (China) and maintained at the Experimental Animal Center of Shandong University (Jinan, China). The animal studies were approved by Stomatological Hospital, Shandong University (Protocol No. GD201903). The experimental procedures were performed following National Institutes of Health guidelines for the care and use of laboratory animals (NIH Publications NO. 8023, revised 1978).

Twenty rats were randomly divided into five groups, including healthy rats without inducing periodontitis (Sham), periodontitis with local application of PBS (*Pg*), periodontitis with local application of 250 μg/mL AgNPs (*Pg*+Ag), periodontitis with local application of 500 μM ebselen (*Pg*+Eb), and periodontitis with local application of AgNPs and ebselen (*Pg*+Ag+Eb).

To induce experimental periodontitis, the rats were anesthetized with isoflurane (RWD, Sugar Land, USA, 5% for anesthesia inducing and 2% for maintaining) during the experimental procedure, and then the 4–0 surgical suture was surrounded and tied on the cervical of the maxillary second molar. Next, 50 μL of *P. gingivalis* suspension was injected into the gingival sulcus around the maxillary second molar every 3 days within 2 weeks.

After two weeks of induction, the experimental periodontitis was established. The sutures were kept for the next 2 weeks because they were critical for plaque accumulation to mimic the chronic inflammation with a consistent bacterial infection. During the treatment period, 20 μL samples were injected into the gingival sulcus around the maxillary second molar every other day for 2 weeks. Then the rats were euthanized with overdose anesthesia, the gingival tissue around the maxillary second molar was immediately removed and conserved in RNALater™ RNA stabilization reagent for animal tissue (Beyotime, Shanghai, China), and the part of maxillae including 3 maxillary molars, heart, liver, spleen, lung and kidney were collected and fixed with 4% paraformaldehyde (PFA, Biosharp, Hefei, China) for 24 h and then preserved in 70% alcohol at 4°C for further experiments.

The collected gingival tissues were ground fully by the manual tissue grinder after being taken from the liquid. The next procedure of RNA extraction and PCR was the same as above mentioned. And the primers for NADPH, IL-6, and IL-1β were listed in Table S2.

The collected maxillae were scanned by Micro-CT (Quantum FX, USA) to analyze alveolar bone loss in vivo (90 kV, 88 μA). The three-dimensional (3D) images were reconstructed following the criteria that the occlusion plane could not be seen from the buccal side and all samples kept the same cervical width of the second molar. The distance from the alveolar bone crest (AB) to the cementoenamel junction (CEJ) was measured by image J, representing the degree of alveolar bone loss.

Then the specimens were demineralized by 10% disodium ethylenediamine tetraacetate (EDTA) with stirring for about 2 months. Afterward, the samples were dehydrated using graded ethanol solutions. After vitrification by dimethyl benzene, the specimen was embedded in paraffin for further acquiring paraffin sections with a thickness of 5 μm. Hematoxylin and eosin (H&E) staining was performed to assess alveolar bone loss. The vertical distance between the CEJ and AB represented bone loss. Tartrate-resistant acid phosphatase (TRAP) staining (Solarbio, China) was performed to assess the number of osteoclasts.

Statistical Analysis

All data were presented as the mean ± standard deviation (SD) and experiments were independently repeated three times. One-way ANOVA and two-way ANOVA were used for statistical analysis. *P* value of less than 0.05 was considered to be statistically significant.

Results and Discussion

Synthesis and Characterization of AgNPs

AgNPs were synthesized using the classic Lee-Meisel method (Figure S1A). The successful synthesis of AgNPs was confirmed by the absorbance peak at 402 nm (Figure S1B). The AgNPs showed uniform spherical shapes (Figure S1C). The DLS revealed that particle sizes were in a range of 10 to 100 nm with 23.36 nm on average, the zeta-potential was −24.75 mV, and the PDI of the colloidal solution was 0.324, which represented moderate dispersity (Figure S1D).

Synergistic Antibacterial Effect of AgNPs and Ebselen on Periodontal Pathogens

S. gordonii, F. nucleatum, and *P. gingivalis* are typical early, bridge, and keystone periodontal pathogens that can co-aggregate with other periodontal pathogens, which contribute to the development of periodontitis.[2] Hence, these three representative pathogens were selected to clarify the antimicrobial characteristics of AgNPs and ebselen. First, the

bactericidal efficacies of AgNPs and ebselen were measured using the CFU counting method. 10 μg/mL AgNPs in this study partially killed *P. gingivalis* and *F. nucleatum*, two Gram-negative bacteria (Figures 1A, B and S2) while showing no effect on *S. gordonii* (Figure S3), the Gram-positive bacteria. This discrepancy may be related to the thicker cell walls of gram-positive bacteria, which are composed of various peptidoglycan coats and thus serve as a barrier for the penetration of the AgNPs.[24] 10 μg/mL AgNPs significantly reduced the viability of *F. nucleatum* while decreasing less effect on *P. gingivalis* (Figures 1A, B, and S2A), which was coincident with Sirisha P's study showing that *P. gingivalis* with higher resistance to AgNPs than *F. nucleatum*.[25]

As expected, when combined with ebselen, especially 10 μM ebselen, the bactericidal efficacy of AgNPs on *P. gingivalis* was significantly enhanced, even 10 μg/mL AgNPs combined with 10 μM ebselen killed 99% *P. gingivalis* within 24 h, indicating AgNPs and ebselen possessed a synergistic bactericidal effect on planktonic *P. gingivalis* (Figure 1A and B), which agreed with the previous study against *Acinetobacter baumannii*.[26] However, the synergistic bactericidal effect of ebselen on *F. nucleatum* was not obvious (Figure S2A), which may be because the more effective antioxidative system in *F. nucleatum* resulted in higher tolerance for oxidative stress than *P. gingivalis*.[27] Encouragingly, the addition of ebselen enhanced the inhibitory effect of AgNPs significantly and prolonged their antibacterial capacity on *P. gingivalis* and *F. nucleatum* for up to 72 h (Figures 1C–E and S2B–D).

The ROS levels in *P. gingivalis*, the keystone pathogen for periodontitis, were detected to further investigate the potential mechanism of the synergistic antibacterial effect of AgNPs and ebselen. Either AgNPs or ebselen induced

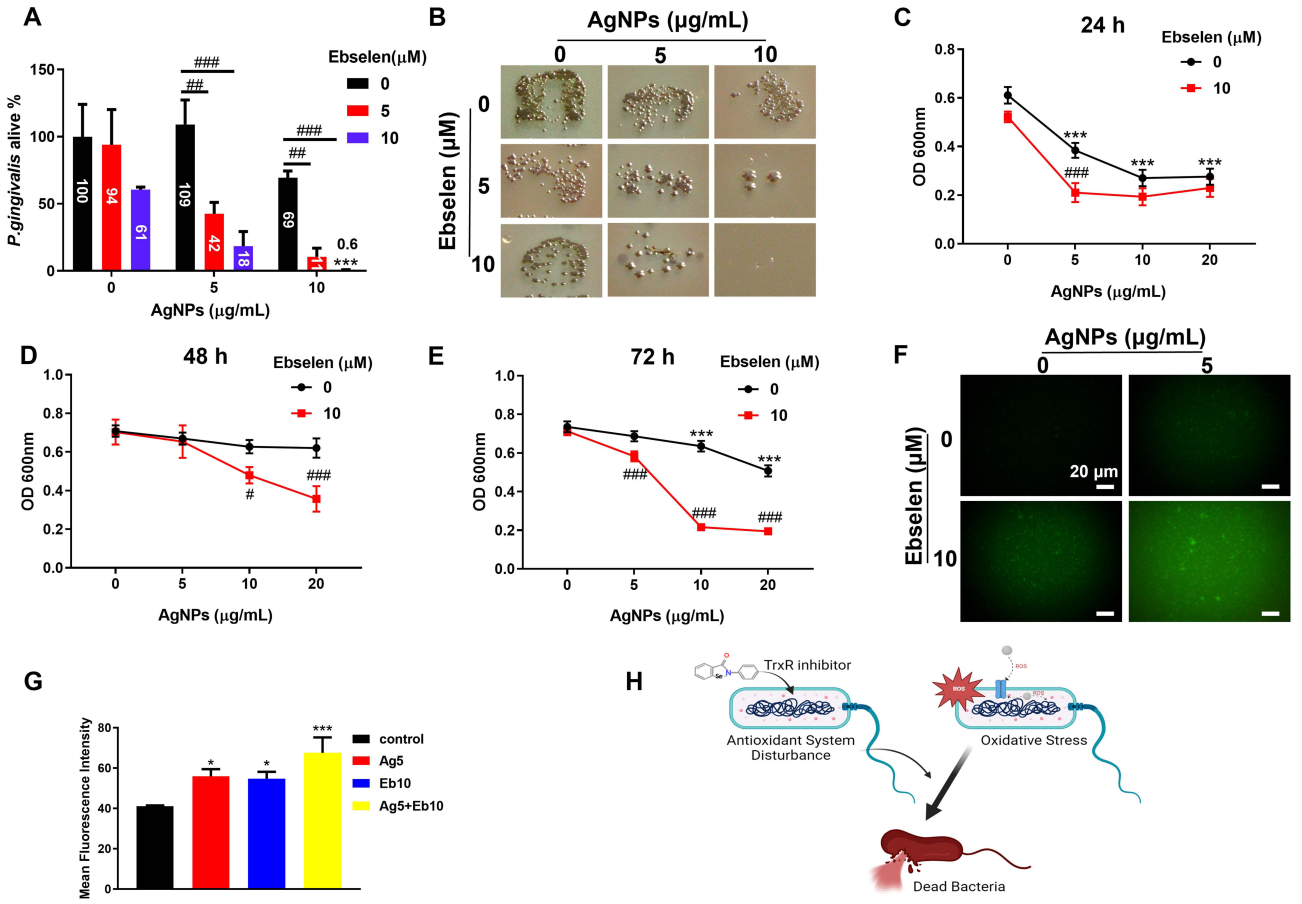

Figure 1 Synergistic antibacterial effect of AgNPs and ebselen on planktonic *P. gingivalis* owing to intracellular ROS increase. (**A** and **B**) CFU counting results of live bacteria after treatment with various concentrations of AgNPs and ebselen for 24 h; (**C–E**) Inhibitory effect of AgNPs and ebselen on *P. gingivalis* growth after treatment for 24, 48, and 72 h, respectively; (**F**) Representative fluorescence images of ROS levels in *P. gingivalis* after being treated with AgNPs and ebselen for 2 h (scale bars: 20 μm); (**G**) The mean fluorescence intensities of ROS levels in *P. gingivalis*; (**H**) Schematic diagram about the potential antibacterial mechanism of AgNPs and ebselen; created with BioRender.com. Data were presented as the mean ± SD. Compared with the control group, $^{*}P < 0.05$, $^{***}P < 0.001$. Compared with the group with the same concentration of AgNPs, $^{\#}P < 0.05$, $^{\#\#}P < 0.01$, $^{\#\#\#}P < 0.001$.

a slight increase in ROS levels, while the combination generated a significantly enhanced increment of ROS level in *P. gingivalis* (Figure 1F and G). The synergistic antibacterial effect of AgNPs and ebselen may be the superimposing result of the enhancement of oxidative systems and dysfunction of the antioxidant system in bacteria (Figure 1H). The released Ag ion inside cells can deactivate the respiratory enzyme and then induce ROS generation.[8] Also, ebselen could also destroy antioxidant function in bacteria by acting as a TrxR inhibitor,[20] and the bacteria with antioxidant system disturbance would be more sensitive to ROS increase.[28]

Anti-Biofilm Effect of AgNPs and Ebselen

Periodontitis is initiated from the bacterial biofilms composed of multispecies communities with heterogeneous structures on the tooth and gingival surfaces. *S. gordonii, F. nucleatum*, and *P. gingivalis* serve as the early, bridge, and late colonizers and contribute to the progress of periodontitis.[2,3] Because of the complex structure, bacteria enclosed in biofilms are more resistant to attack from the host immune system and antibiotics.[14,29] To this end, the anti-biofilm effects of AgNPs and ebselen were firstly explored against the keystone bacteria, ie, *P. gingivalis*. 5 μg/mL AgNPs showed slight inhibition on biofilm development, and a higher concentration, ie, 10 μg/mL AgNPs inhibited the biofilm-developing more effectively as shown with smaller and thinner biofilm structure (Figure 2A–C). However, AgNPs alone, especially in low concentrations, failed to destroy established biofilms, showing large patches of biofilms with close connections (Figure 2D and E). There were more dead and ruptured bacteria in the biofilms treated with 10 μg/mL AgNPs (Figure 2D and E), which could be attributed to the ability of AgNPs to penetrate biofilms shown in the energy dispersive spectroscopy (EDS) result (Figure 2F), possibly by aquaporin.[30] The penetrated AgNPs could interact with polysaccharides, proteins, and nucleic acid to further destroy biofilm structure.[31] Meanwhile, 10 μM ebselen alone suppressed the development of biofilm significantly, which agreed with the previous study that reported ebselen inhibited the biofilm formation of some drug-resistance bacteria and destroyed established biofilms,[32,33] possibly by inhibiting bacterial protein synthesis.[33] Furthermore, the combination of AgNPs and ebselen showed more obvious anti-biofilm effects on both biofilm formation and eradication, manifesting as the biofilms were looser and thinner with more dead bacteria according to the result of SEM and CLSM images (Figure 2A–E). Besides, the evaluation of the anti-biofilm effect on *F. nucleatum* or *S. gordonii* showed similar results as the combination of AgNPs and ebselen presented a great antibiofilm effect regardless of the type of bacteria (Figure 3).

To better simulate the establishment of the complex biofilm, a mixture of *S. gordonii, F. nucleatum*, and *P. gingivalis* was further created to evaluate the anti-biofilm effect. There was a high proportion of live bacteria adhered on the surface in the control group, while 5 and 10 μg/mL AgNPs treatment groups displayed more dead bacteria (Figure 4A and B). With the treatment of 10 μM ebselen, smaller biofilm structures with thinner layers were established (Figure 4A–C), this further clarified the inhibitory effect of ebselen on biofilm formation. Possibly, ebselen impeded biofilm establishment by inhibiting the function of cyclic-di-GMP (cdiGMP), which is an important second messenger to regulate biofilm formation.[34,35] The AgNPs and ebselen combination resulted in biofilms with more dead bacteria and thinner layers, which further corroborated the excellent inhibitory effects on biofilm formation (Figure 4A–C). The crystal violet staining result showed a similar tendency as previously described (Figure 4D). Surprisingly, the combination of AgNPs and ebselen also demonstrated excellent efficacy in biofilm eradication (Figure 4E and F). The thickness of multispecies biofilms was reduced from 15 μm (mean of the control group) to 9.33 μm (mean of 5 μg/mL AgNPs and 10 μM ebselen group) and 8 μm (mean of 10 μg/mL AgNPs and 10 μM ebselen group), respectively (Figure 4G). In addition, the crystal violet staining result also proved the excellent dispersive effect of AgNPs and ebselen combination on multispecies biofilms (Figure 4H). The synergistic anti-biofilm effect could be attributed to both the inhibition effect from ebselen, which suppressed the establishment of fresh biofilms by inhibiting the synthesis of protein, and the destructive effect from AgNPs, which disrupted the established structures by penetrating inside biofilms (Figure 4I).

In clinic, with the assistance of some macromolecules, such as nucleic acids, proteins, and lipids, the pathogenic bacteria adhere and aggregate on the tooth surfaces to form bacterial biofilms.[36,37] The biofilm formation and dental plaque accumulation are typical manifestations of periodontitis at the initial stage.[38] The removal of biofilm and plaque would contribute to reconstructing the inflammatory homeostasis of the periodontal tissue. Our results showed that the combination of AgNPs and ebselen held excellent synergistic anti-biofilm effect on *S. gordonii, F. nucleatum, P. gingivalis*, and the bacterial mixtures, which may indicate their great potential to assist to prevent and treat periodontitis.

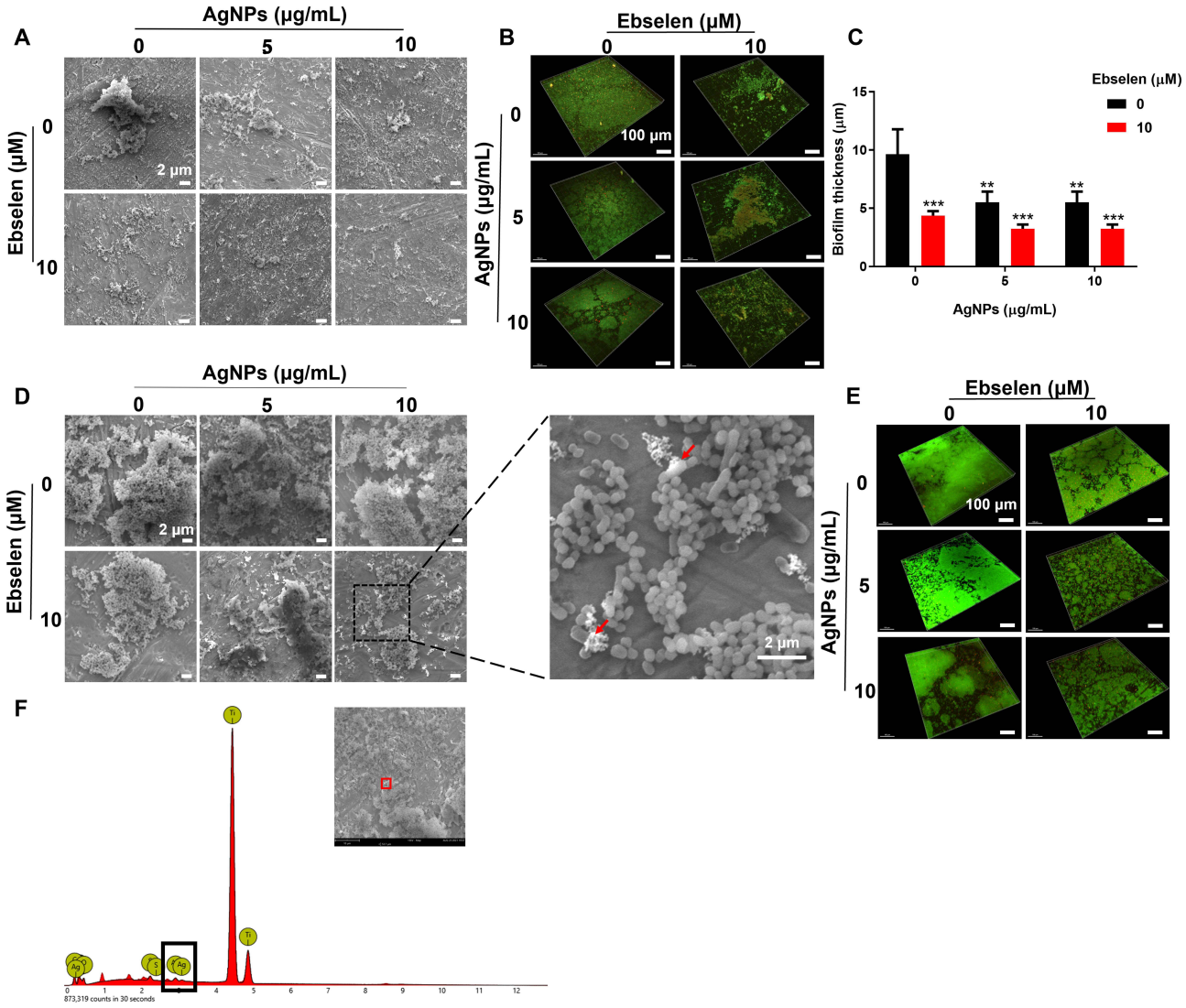

Figure 2 Synergistic anti-biofilm effect of AgNPs and ebselen on *P. gingivalis*. (**A**) SEM images and (**B**) CLSM images of the biofilm formation experiment; (**C**) Biofilm thickness quantified by CLSM; (**D**) SEM images and (**E**) CLSM images of the biofilm destruction experiment, the red arrow in SEM images indicated ruptured *P. gingivalis*; (**F**) EDS result of destructed biofilm. Scale bars in SEM images: 2 μm, scale bars in CLSM images: 100 μm. Data were presented as the mean ± SD. Compared with the control group, $^{**}P < 0.01$, $^{***}P < 0.001$.

Intracellular Bacterial Killing Efficacy of AgNPs and Ebselen

Surviving within cells is another way for *P. gingivalis* to escape from immune surveillance and avoid the bactericidal effect of antibiotics.[39,40] AgNPs have been reported with the ability to diminish intracellular bacteria, but 5–10 μg/mL AgNPs did not show significant antibacterial effects against intracellular *P. gingivalis* (Figure 5A and B), possibly because the entry of AgNPs into cells was relatively slow. For the synthesized AgNPs with an average particle size of 23.36 nm (Figure S1D), Wu et al demonstrated that there was only a cellular uptake efficiency of approximately 22% for AgNPs in 20 nm size,[41] resulting in fewer AgNPs inside to exert antibacterial effects. When combined with ebselen, 5 μg/mL AgNPs diminished intracellular *P. gingivalis* by approximately 50%, and 10 μg/mL AgNPs killed around 90% of intracellular bacteria (Figure 5A). Otherwise, the enhanced intracellular antibacterial effects were further proved by detecting the CFSE-DA labeled *P. gingivalis* inside HGFs (Figure 5B). Although ebselen has a weak antibacterial effect, it can enter cells rapidly with the uptake reaching the peak after 2 h.[42] Hence, the accumulated ebselen inside could be responsible for the enhanced antibacterial effect of AgNPs, which reduced the effective concentration of AgNPs significantly (Figure 5C).

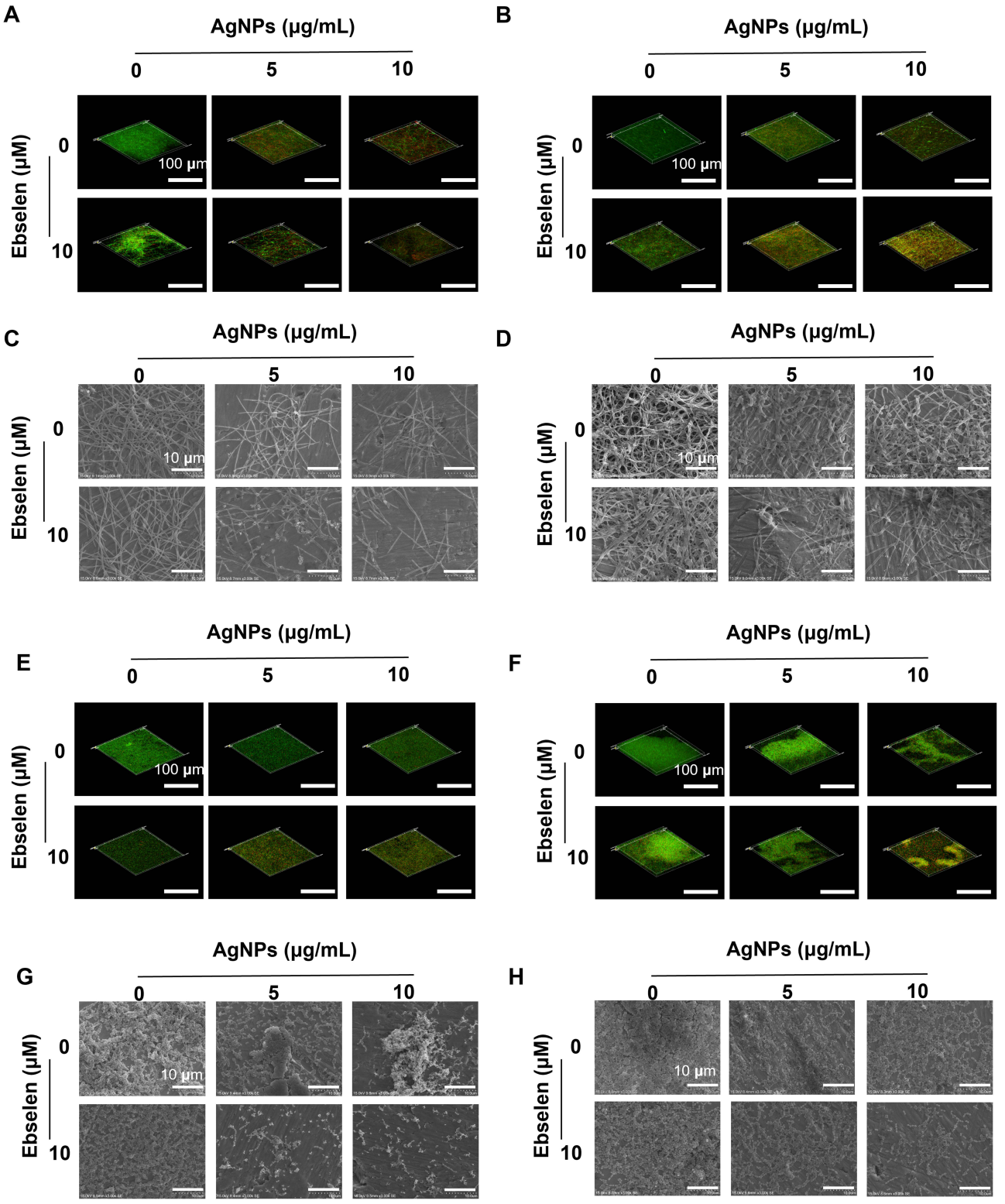

Figure 3 Synergistic anti-biofilm effect of AgNPs and ebselen on *F. nucleatum* and *S. gordonii*. CLSM images of the biofilm formation experiment (**A**) and the biofilm destruction experiment (**B**) on *F. nucleatum*; SEM images of the biofilm formation experiment (**C**) and the biofilm destruction experiment (**D**) on *F. nucleatum*; CLSM images of the biofilm formation experiment (**E**) and the biofilm destruction experiment (**F**) on *S. gordonii*; SEM images of the biofilm formation experiment (**G**) and the biofilm destruction experiment (**H**) on *S. gordonii*. Scale bars in CLSM images: 100 μm, scale bars in SEM images: 10 μm.

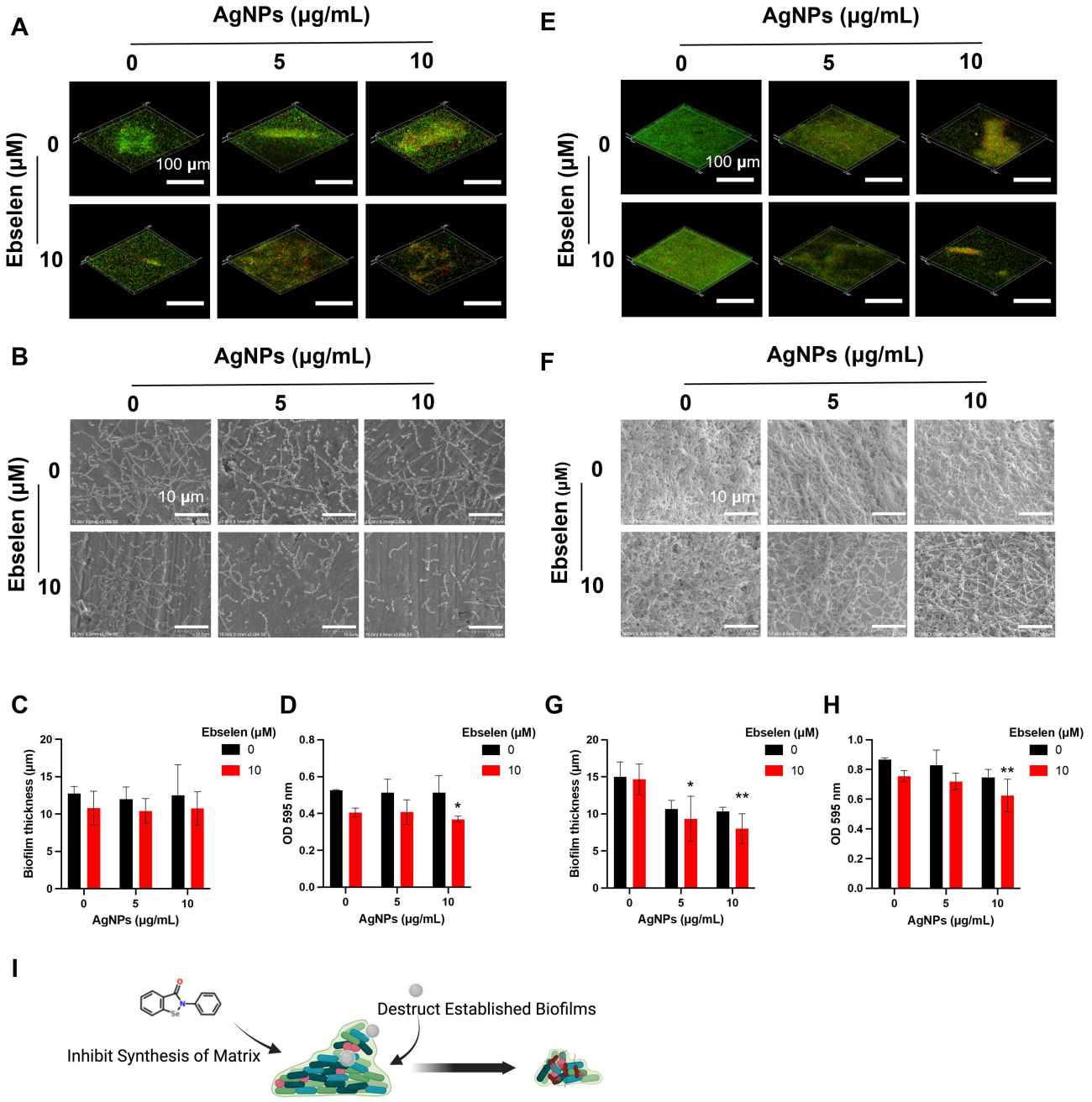

Figure 4 Synergistic anti-biofilm effect of AgNPs and ebselen on multispecies biofilms. (**A**) CLSM images and (**B**) SEM images of the biofilm formation experiment; (**C**) Biofilm thickness of the biofilm formation experiment quantified by CLSM; (**D**) The crystal violet staining result of the biofilm formation experiment; (**E**) CLSM images and (**F**) SEM images of the biofilm destruction experiment; (**G**) Biofilm thickness of the biofilm destruction experiment quantified by CLSM; (**H**) The crystal violet staining result of the biofilm destruction experiment; (**I**) The schematic diagram about the potential antibiofilm mechanism of AgNPs and ebselen; created with BioRender.com. Scale bars in CLSM images: 100 μm, scale bars in SEM images: 10 μm. Data were presented as the mean ± SD. Compared with the control group, $^{*}P < 0.05$, $^{**}P < 0.01$.

Cell Proliferation and Intracellular ROS Levels of HGFs Treated with AgNPs and Ebselen

Besides antibacterial properties, cytocompatibility is pivotal for the potential in biomedical applications. CCK-8 result showed that either alone or combined application of up to 20 μg/mL AgNPs and 10 μM ebselen had no disturbance on cell proliferation (Figure 6A). However, AgNPs treatment shifted the peak of fluorescence intensity to the right compared with the control group at 6 h and the tendency became more obvious at 24 h, indicating that intracellular ROS increased with time (Figure 6B). When AgNPs were applied together with 10 μM ebselen, the peak shifted to the left, meaning the

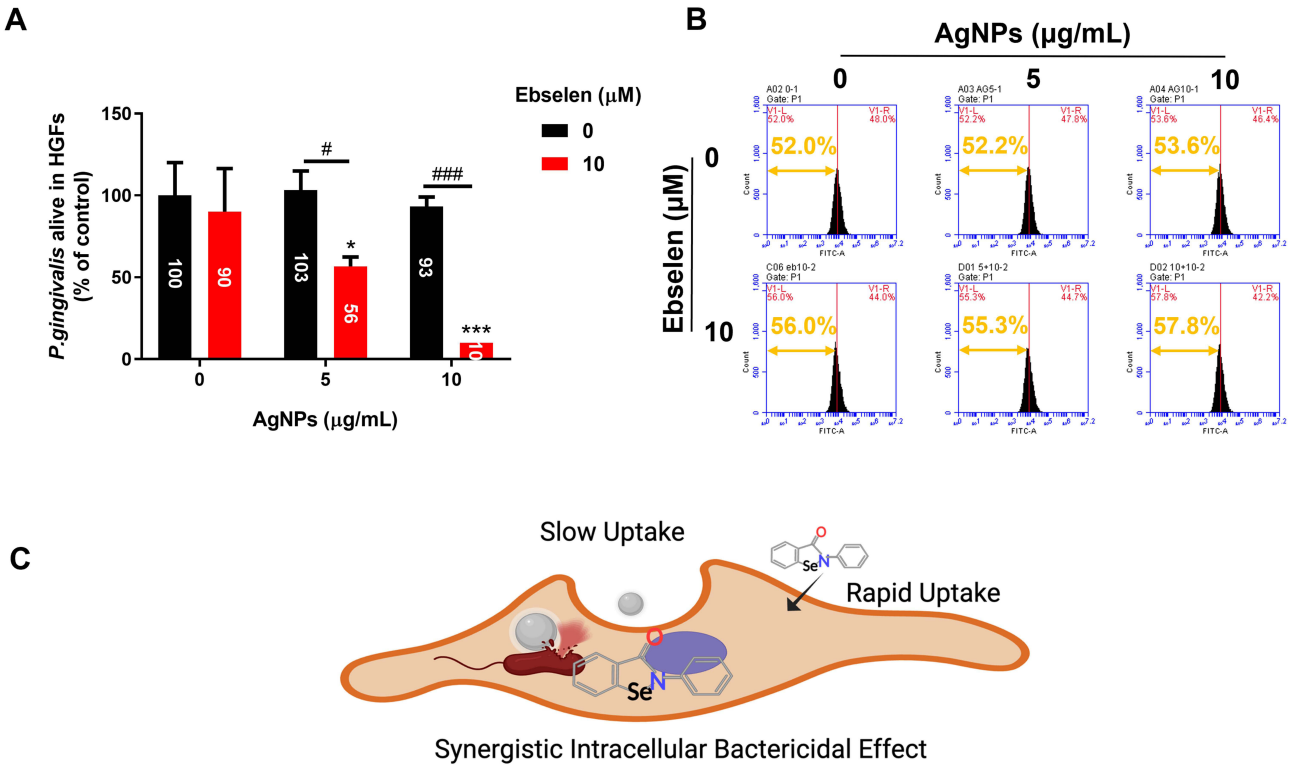

Figure 5 Intracellular bactericidal efficacies of AgNPs and ebselen. (**A**) Viability of *P. gingivalis* inside HGFs; (**B**) The fluorescence intensity of HGFs infected with CFDA-SE labeled *P. gingivalis* in different groups; (**C**) The schematic diagram about the potential mechanism of synergistic intracellular bactericidal effect of AgNPs and ebselen; created with BioRender.com. Data were presented as the mean ± SD. Compared with the control group, $^{*}P < 0.05$, $^{***}P < 0.001$. Compared with the group with the same concentration of AgNPs, $^{\#}P < 0.05$, $^{\#\#\#}P < 0.001$.

addition of ebselen recovered ROS equilibrium to protect HGFs from oxidative injury (Figure 6B). The representative fluorescence photos and the quantitative mean fluorescence intensities exhibited a similar trend (Figure 6C and D). To further explore the potential mechanism of ebselen relieving AgNPs-induced oxidative stress, the key enzymes of antioxidant systems including GSH, TrxR, and SOD2 were evaluated.[43–45] The thiol groups are active points of the GSH and Trx antioxidant system, which are also the binding target of AgNPs and the released silver ions,[17] thus these antioxidative enzymes were detected. 5 μg/mL AgNPs alone reduced the total amount of GSH, while combined with ebselen, the GSH amount bounced back (Figure 6E). Hence, the incremental GSH was utilized by ebselen, a GSH-Px mimic, to promote the elimination of intracellular ROS.[42] Meanwhile, AgNPs also inhibited TrxR activity significantly, but the addition of ebselen failed to recover it despite ebselen alone did it (Figure 6F), indicating that ebselen, as the substrate of mammalian TrxR and Trx, cannot reverse the inactivation of TrxR caused by binding of AgNPs.[42] Moreover, SOD2, a key enzyme scavenging mitochondrial ROS, was upregulated by AgNPs and/or ebselen while the combined application of AgNPs and ebselen boosted SOD2 expression synergistically (Figure 6G). Consequently, the oxidative and anti-oxidative activities in HGFs treated with AgNPs and ebselen may have reached a balance and thus protect the cells from oxidative damage (Figure 6H).

Anti-Inflammatory Effect of AgNPs and Ebselen on *P. gingivalis*-Infected HGFs

To further explore the anti-inflammatory effect of AgNPs and ebselen, *P. gingivalis*-infected HGFs were treated with 5 μg/mL AgNPs and 10 μM ebselen, either alone or combined (Figure 7A). As a result, *P. gingivalis* dramatically upregulated the expression of pro-inflammatory cytokine IL-6, IL-8, and CCL2 at both mRNA and secretory protein levels (Figure 7B and C). When treated with AgNPs or ebselen alone, the pro-inflammatory cytokines decreased only at mRNA levels, but there was still a high concentration of inflammatory factors secreted (Figure 7B and C). Indeed, these inflammatory cytokines declined obviously at both mRNA and protein levels when treated with the combination of AgNPs and ebselen, indicating AgNPs and ebselen held anti-inflammatory effects and could protect cells from *P. gingivalis* infection (Figure 7B and C). Regarding

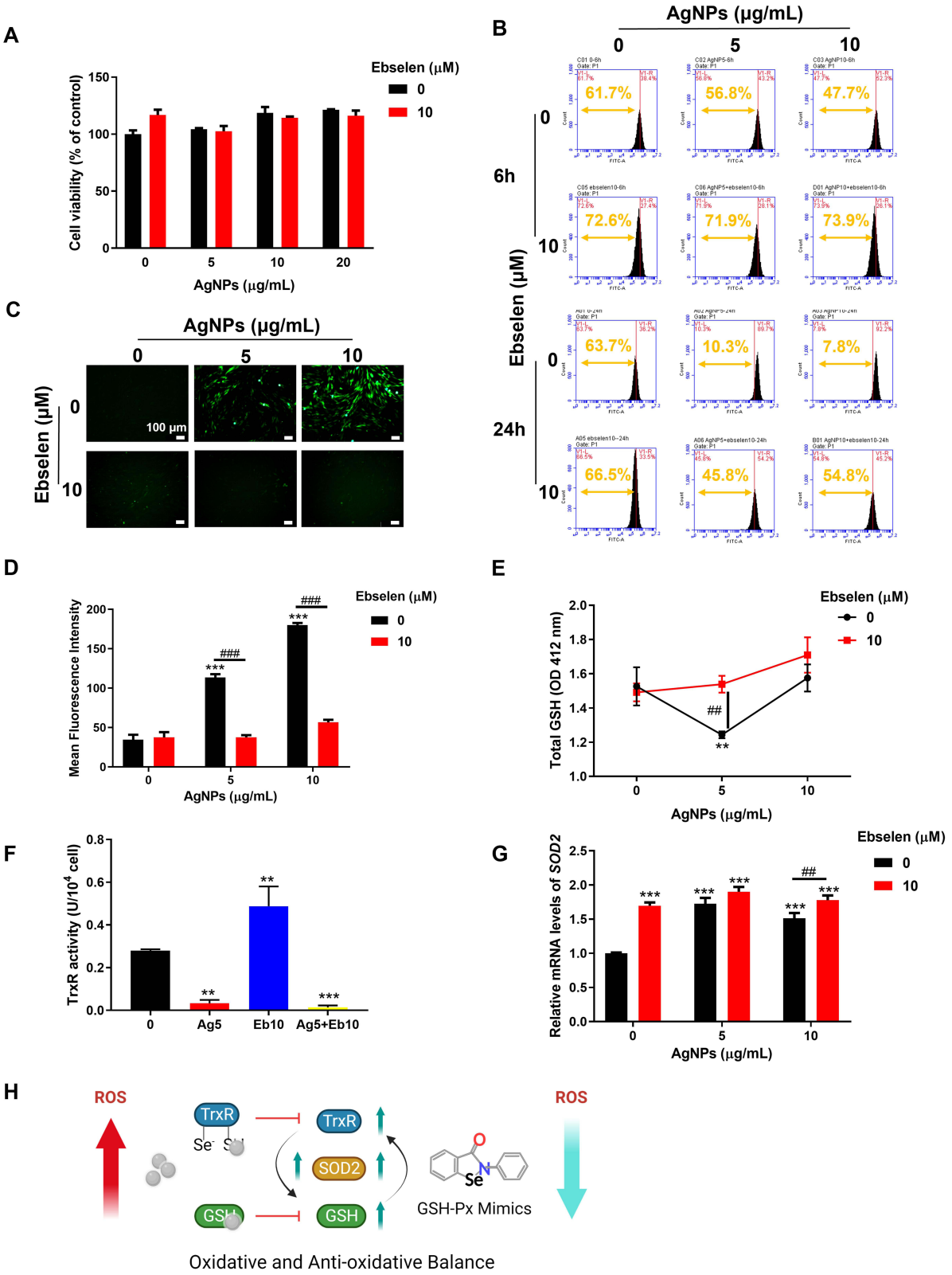

Figure 6 Cell viability and intracellular ROS levels of HGFs treated with AgNPs and ebselen. (**A**) Cell viability of HGFs treated with AgNPs and ebselen; (**B**) Intracellular ROS levels of HGFs in treatment with AgNPs and ebselen for 6 and 24 h; (**C**) Fluorescence images were taken at 24 h (scale bars: 100 μm), and (**D**) the mean fluorescence intensities were measured by image J; (**E**) The amount of total GSH in HGFs; (**F**) TrxR activities in HGFs; (**G**) Expression of SOD2 in HGFs; (**H**) The schematic illustration of the effect of AgNPs and ebselen on anti-oxidative system; created with BioRender.com. Data were presented as the mean ± SD. Compared with the control group, $^{**}P < 0.01$, $^{***}P < 0.001$. Compared with the group with the same concentration of AgNPs, $^{\#\#}P < 0.01$, $^{\#\#\#}P < 0.001$.

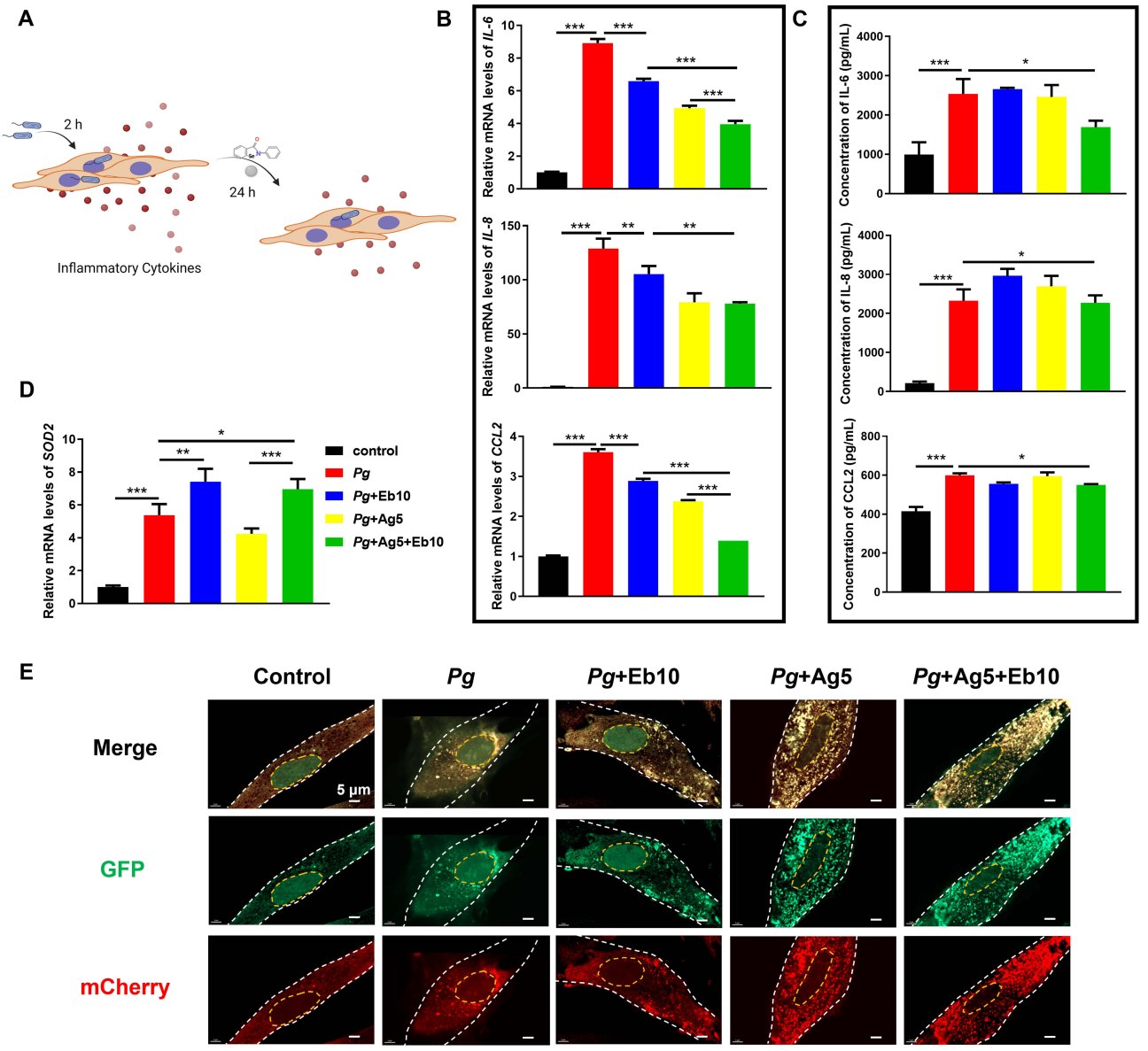

Figure 7 Anti-inflammatory effect of AgNPs and ebselen on *P. gingivalis*-infected HGFs. (**A**) The schematic diagram for the application of AgNPs and ebselen in *P. gingivalis*-infected HGFs, created with BioRender.com; (**B**) Relative mRNA and (**C**) protein expression levels of IL-6, IL-8, and CCL2 in *P. gingivalis*-infected HGFs; (**D**) Relative expression of SOD2 mRNA in *P. gingivalis*-infected HGFs; (**E**) Autophagic flux in *P. gingivalis*-infected HGFs with the treatment of AgNPs and ebselen (scale bars: 5 μm). Data were presented as the mean ± SD. **P* < 0.05, ***P* < 0.01, ****P* < 0.001.

SOD2, an opposite tendency was exhibited, whose expression was upregulated in both ebselen groups and the combined group for alleviating oxidative stress (Figure 7D). Furthermore, as both *P. gingivalis* and AgNPs can be scavenged by autophagy which might be beneficial for relieving bacterial infection,[12] we further evaluated the autophagic levels in HGFs by staining autophagosome in yellow puncta and autolysosome in red puncta. Ebselen alone showed little effect on cellular autophagy; however, AgNPs alone group and the combined group significantly enhanced cellular autophagy in *P. gingivalis*-infected HGFs (Figure 7E). Meanwhile, ebselen played an anti-inflammatory role by inhibiting nuclear factor-κB and mitogen-activated protein kinase signaling pathways activation.[46] Consequently, the synergistic anti-inflammatory effects were attributed to AgNPs promoting scavenging of hazardous factors and ebselen inhibiting inflammatory factors expression.

Effect of AgNPs and Ebselen on Rat Experimental Periodontitis

The therapeutic effects of AgNPs and ebselen were further evaluated in a rat periodontitis model in vivo. The rat experimental periodontitis was successfully constructed by ligature with *P. gingivitis* Infection locally (Figure S4A).

Generally, all rats experienced similar weight increases (Figure S4B), and the blood routine examination showed no alteration in red blood cells (RBC), white blood cells (WBC), and platelets (PLT) (Figure S4C–E). The histopathological examination of the main visceral organs revealed no obvious abnormal manifestation in the heart, liver, spleen, lung, and kidney in all groups (Figure S4F).

P. gingivitis with other periodontal pathogens accumulated around the teeth and established biofilms, thus inducing host immune defense and inflammatory response.[47] *P. gingivalis* stimulation caused severe inflammation by showing significantly enhanced expression of IL-1β and IL-6 (Figure 8A and B). The longer epithelial ridge of epithelium and more inflammatory cell infiltration also demonstrated the accumulated inflammation in the gingival tissue (Figure 8C). With treatment of AgNPs and ebselen, either alone or combined, significantly decreased the expression of inflammatory cytokines in gingival tissues (Figure 8A and B) and reduced inflammatory cell infiltration (Figure 8C). There was no additional anti-inflammatory effect observed in the combined group, which could be the consequence that AgNPs or ebselen alone already diminished the residual bacterial burden in the experimental settings efficiently. Furthermore, the treatment of AgNPs and ebselen, either alone or together, alleviated marginal alveolar bone resorption obviously compared with *P. gingivalis*-infected control group (Figure 8C–F). Consistently, further osteoclast staining and enumeration revealed that TRAP-positive cells in all AgNPs and ebselen groups were significantly less than *P. gingivalis*-infected control group (Figure 8G and H). The in vivo study demonstrated that the combined application of AgNPs and ebselen would be an efficient strategy for periodontitis based on reduced gingival inflammation and alveolar bone absorption.

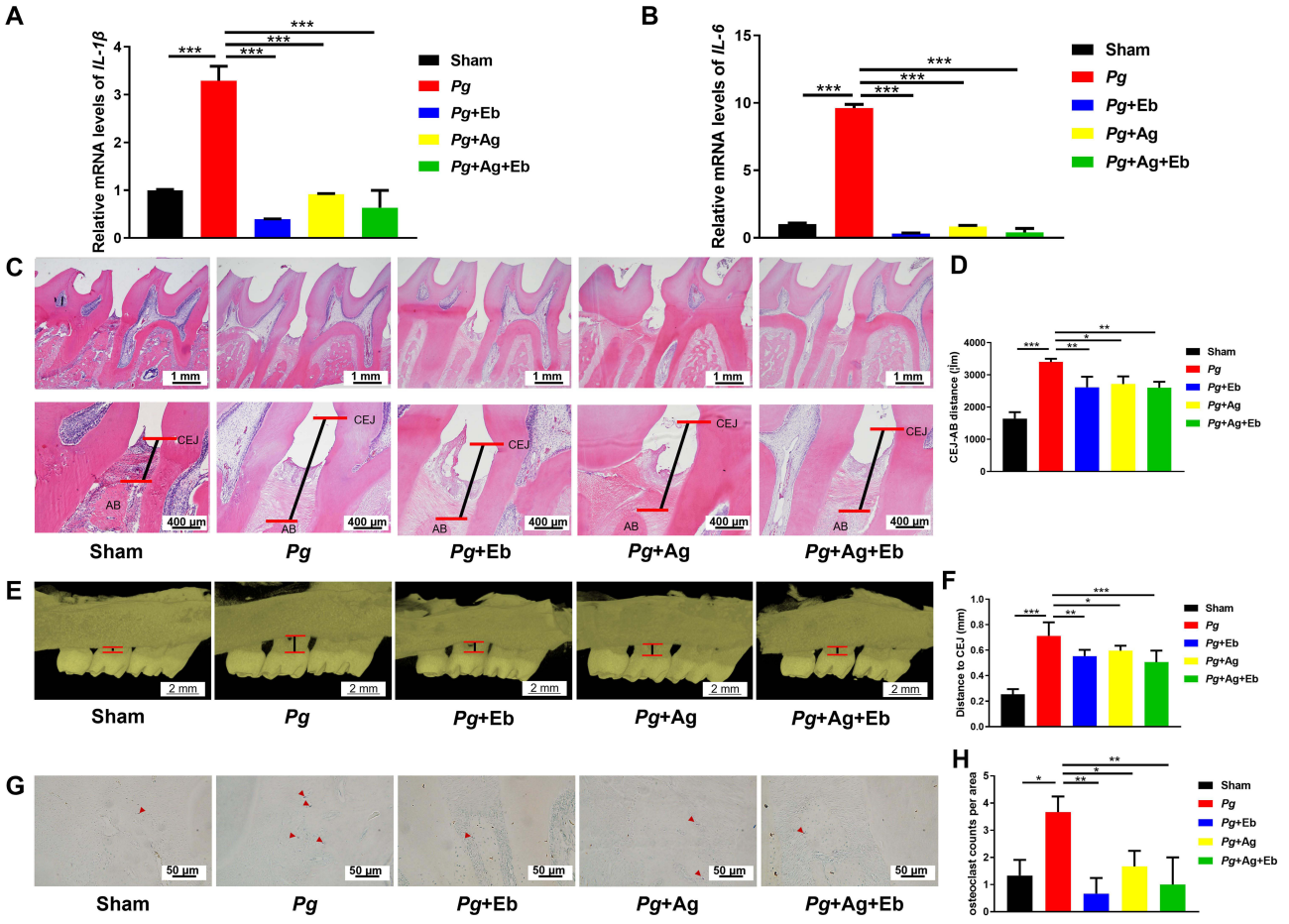

Figure 8 Effect of AgNPs and ebselen on rat experimental periodontitis. (**A** and **B**) The relative mRNA expression levels of IL-1β and IL-6 in gingival tissues; (**C** and **D**) The marginal bone resorption of alveolar bone in H&E staining images; (**E** and **F**) The marginal bone resorption of alveolar bone by Micro-CT evaluation; (**G** and **H**) The representative photos and quantification of osteoclasts in TRAP staining images; the red arrows indicated TRAP$^+$ cells. Data were presented as the mean ± SD. **P* < 0.05, ***P* < 0.01, ****P* < 0.001.

Conclusion

AgNPs and ebselen showed synergistic anti-biofilm effects on *S. gordonii, F. nucleatum, P. gingivalis*, and the bacterial mixtures, and thus reduced therapeutic threshold concentrations of AgNPs. The combination held excellent cytocompatibility, reduced intracellular oxidative stress, and anti-inflammatory effects, which were related to the reduction of intracellular oxidative stress by increasing GSH content and mitochondrial SOD2 expression. In vivo, AgNPs and ebselen combination could reduce alveolar bone resorption. Therefore, the combined application of AgNPs and ebselen would be a promising treatment strategy for periodontitis.

Acknowledgments

Figure 1H, Figure 4I, Figure 5C, Figure 6H, Figure 7A, graphical abstract, and Figure S1A were drawn by Biorender (www.biorender.com).

Funding

This work was supported by the National Natural Science Foundation of China (No. 81901009, 82170964, and 81873716), China Postdoctoral Science Foundation (No. 2019M652409, No. 2021TQ0194, and No. 2022M711906), the Construction Engineering Special Fund of "Taishan Scholars" of Shandong Province (No.ts20190975 and No. tsqn202211325), Shandong Province Key Research and Development Program (No. 2021ZDSYS18), Shandong Province Major Scientific and Technical Innovation Project (No. 2021SFGC0502), Guangdong Basic and Applied Basic Research Foundation (No. 2020A1515110851), Shandong Provincial Natural Science Foundation (No. ZR2021QH225), and COS Basic Research Fund (No. COS-B2021-10).

Disclosure

The authors report no conflicts of interest in this work.

References

1. Slots J. Periodontitis: facts, fallacies and the future. *Periodontol 2000*. 2017;75(1):7–23. doi:10.1111/prd.12221
2. Park OJ, Kwon Y, Park C, et al. Streptococcus gordonii: pathogenesis and host response to its cell wall components. *Microorganisms*. 2020;8(12):1852. doi:10.3390/microorganisms8121852
3. Yang R, Liu T, Pang C, et al. The regulatory effect of coaggregation between Fusobacterium nucleatum and Streptococcus gordonii on the synergistic virulence to human gingival epithelial cells. *Front Cell Infect Microbiol*. 2022;12:879423. doi:10.3389/fcimb.2022.879423
4. Sakanaka A, Kuboniwa M, Shimma S, et al. Fusobacterium nucleatum metabolically integrates commensals and pathogens in oral biofilms. *mSystems*. 2022;7(4):e0017022. doi:10.1128/msystems.00170-22
5. Bostanci N, Belibasakis GN. Porphyromonas gingivalis: an invasive and evasive opportunistic oral pathogen. *FEMS Microbiol Lett*. 2012;333(1):1–9. doi:10.1111/j.1574-6968.2012.02579.x
6. Sakanaka A, Takeuchi H, Kuboniwa M, Amano A. Dual lifestyle of Porphyromonas gingivalis in biofilm and gingival cells. *Microb Pathog*. 2016;94:42–47. doi:10.1016/j.micpath.2015.10.003
7. Ardila CM, Bedoya-Garcia JA. Antimicrobial resistance of Aggregatibacter actinomycetemcomitans, Porphyromonas gingivalis and Tannerella forsythia in periodontitis patients. *J Glob Antimicrob Resist*. 2020;22:215–218. doi:10.1016/j.jgar.2020.02.024
8. Yin IX, Zhang J, Zhao IS, Mei ML, Li Q, Chu CH. The antibacterial mechanism of silver nanoparticles and its application in dentistry. *Int J Nanomed*. 2020;15:2555–2562. doi:10.2147/IJN.S246764
9. Siddiqi KS, Husen A, Rao RAK. A review on biosynthesis of silver nanoparticles and their biocidal properties. *J Nanobiotechnol*. 2018;16(1):14. doi:10.1186/s12951-018-0334-5
10. Emmanuel R, Palanisamy S, Chen SM, et al. Antimicrobial efficacy of green synthesized drug blended silver nanoparticles against dental caries and periodontal disease causing microorganisms. *Mater Sci Eng C Mater Biol Appl*. 2015;56:374–379. doi:10.1016/j.msec.2015.06.033
11. Kang J, Dietz MJ, Hughes K, Xing M, Li B. Silver nanoparticles present high intracellular and extracellular killing against Staphylococcus aureus. *J Antimicrob Chemother*. 2019;74(6):1578–1585. doi:10.1093/jac/dkz053
12. Sharma S, Tiwari M, Tiwari V. Therapeutic strategies against autophagic escape by pathogenic bacteria. *Drug Discov Today*. 2021;26(3):704–712. doi:10.1016/j.drudis.2020.12.002
13. Markowska K, Grudniak A, Wolska KI. Silver nanoparticles as an alternative strategy against bacterial biofilms. *Acta Biochim Pol*. 2013;60(4):523–530.
14. Palanisamy NK, Ferina N, Amirulhusni AN, et al. Antibiofilm properties of chemically synthesized silver nanoparticles found against Pseudomonas aeruginosa. *J Nanobiotechnology*. 2014;12(1):2. doi:10.1186/1477-3155-12-2
15. Palacios-Hernandez T, Diaz-Diestra DM, Nguyen AK, et al. Cytotoxicity, cellular uptake and apoptotic responses in human coronary artery endothelial cells exposed to ultrasmall superparamagnetic iron oxide nanoparticles. *J Appl Toxicol*. 2020;40(7):918–930. doi:10.1002/jat.3953
16. Lu J, Holmgren A. The thioredoxin antioxidant system. *Free Radic Biol Med*. 2014;66:75–87. doi:10.1016/j.freeradbiomed.2013.07.036

17. Jiang HS, Zhang Y, Lu ZW, Lebrun R, Gontero B, Li W. Interaction between Silver Nanoparticles and Two Dehydrogenases: role of Thiol Groups. *Small*. 2019;15(27):e1900860. doi:10.1002/smll.201900860
18. Bustos PS, Quinteros MLA, Gomez DS, Ortega MG, Paez PL, Guinazu NL. Silver bionanoparticles toxicity in trophoblast is mediated by nitric oxide and glutathione pathways. *Toxicology*. 2021;454:152741. doi:10.1016/j.tox.2021.152741
19. Ren X, Zou L, Lu J, Holmgren A. Selenocysteine in mammalian thioredoxin reductase and application of ebselen as a therapeutic. *Free Radic Biol Med*. 2018;127:238–247. doi:10.1016/j.freeradbiomed.2018.05.081
20. Zou L, Lu J, Wang J, et al. Synergistic antibacterial effect of silver and ebselen against multidrug-resistant Gram-negative bacterial infections. *EMBO Mol Med*. 2017;9(8):1165–1178. doi:10.15252/emmm.201707661
21. Chen X, Chen H, Zhang H, et al. Characterization of synergistic antibacterial effect of silver nanoparticles and ebselen. *Artif Cells Nanomed Biotechnol*. 2019;47(1):3338–3349. doi:10.1080/21691401.2019.1648278
22. Wan Y, Guo Z, Jiang X, et al. Quasi-spherical silver nanoparticles: aqueous synthesis and size control by the seed-mediated Lee-Meisel method. *J Colloid Interface Sci*. 2013;394:263–268. doi:10.1016/j.jcis.2012.12.037
23. Kang W, Shang L, Wang T, Liu H, Ge S. Rho-kinase inhibitor Y-27632 downregulates LPS-induced IL-6 and IL-8 production via blocking p38 MAPK and NF-kappaB pathways in human gingival fibroblasts. *J Periodontol*. 2018;89(7):883–893. doi:10.1002/JPER.17-0571
24. Anees Ahmad S, Sachi Das S, Khatoon A, et al. Bactericidal activity of silver nanoparticles: a mechanistic review. *Mater Sci Energy Technol*. 2020;3:756–769. doi:10.1016/j.mset.2020.09.002
25. Amulya SD KS, Gayathri GV, S P. Antimicrobial effect of silver-nanoparticles synthesised with Ocimum sanctum leaf extract on periodontal pathogens. *J Oral Health Dent Sci*. 2017;1(1):7.
26. Dong C, Wang J, Chen H, et al. Synergistic therapeutic efficacy of ebselen and silver ions against multidrug-resistant Acinetobacter baumannii-induced urinary tract infections. *Metallomics*. 2020;12(6):860–867. doi:10.1039/d0mt00091d
27. Diaz PI, Zilm PS, Rogers AH. Fusobacterium nucleatum supports the growth of Porphyromonas gingivalis in oxygenated and carbon-dioxide-depleted environments. *Microbiology*. 2002;148(Pt2):5. doi:10.1099/00221287-148-2-467
28. Dharmaraja AT. Role of Reactive Oxygen Species (ROS) in therapeutics and drug resistance in cancer and bacteria. *J Med Chem*. 2017;60 (8):3221–3240. doi:10.1021/acs.jmedchem.6b01243
29. Kariu T, Nakao R, Ikeda T, Nakashima K, Potempa J, Imamura T. Inhibition of gingipains and Porphyromonas gingivalis growth and biofilm formation by prenyl flavonoids. *J Periodontal Res*. 2017;52(1):89–96. doi:10.1111/jre.12372
30. Liu Y, Shi L, Su L, et al. Nanotechnology-based antimicrobials and delivery systems for biofilm-infection control. *Chem Soc Rev*. 2019;48 (2):428–446. doi:10.1039/c7cs00807d
31. Joshi AS, Singh P, Mijakovic I. Interactions of gold and silver nanoparticles with bacterial biofilms: molecular interactions behind inhibition and resistance. *Int J Mol Sci*. 2020;21(20):7658. doi:10.3390/ijms21207658
32. AbdelKhalek A, Abutaleb NS, Mohammad H, Seleem MN, Chang Y-F. Repurposing ebselen for decolonization of vancomycin-resistant enterococci (VRE). *PLoS One*. 2018;13(6):e0199710. doi:10.1371/journal.pone.0199710
33. Thangamani S, Younis W, Seleem MN. Repurposing ebselen for treatment of multidrug-resistant staphylococcal infections. *Sci Rep*. 2015;5 (1):11596. doi:10.1038/srep11596
34. Gursoy UK, Gursoy M, Kononen E, Sintim HO. Cyclic dinucleotides in oral bacteria and in oral biofilms. *Front Cell Infect Microbiol*. 2017;7:273. doi:10.3389/fcimb.2017.00273
35. Lieberman OJ, Orr MW, Wang Y, Lee VT. High-throughput screening using the differential radial capillary action of ligand assay identifies ebselen as an inhibitor of diguanylate cyclases. *ACS Chem Biol*. 2014;9(1):183–192. doi:10.1021/cb400485k
36. Herrera D, Alonso B, Leon R, Roldan S, Sanz M. Antimicrobial therapy in periodontitis: the use of systemic antimicrobials against the subgingival biofilm. *J Clin Periodontol*. 2008;35(8 Suppl):45–66. doi:10.1111/j.1600-051X.2008.01260.x
37. Jakubovics NS, Goodman SD, Mashburn-Warren L, Stafford GP, Cieplik F. The dental plaque biofilm matrix. *Periodontol 2000*. 2021;86(1):32–56. doi:10.1111/prd.12361
38. Bartold PM, Van Dyke TE. An appraisal of the role of specific bacteria in the initial pathogenesis of periodontitis. *J Clin Periodontol*. 2019;46 (1):6–11. doi:10.1111/jcpe.13046
39. Zheng S, Yu S, Fan X, et al. Porphyromonas gingivalis survival skills: immune evasion. *J Periodontal Res*. 2021;56(6):1007–1018. doi:10.1111/jre.12915
40. Lin J, Huang D, Xu H, Zhan F, Tan X. Macrophages: a communication network linking Porphyromonas gingivalis infection and associated systemic diseases. *Front Immunol*. 2022;13:952040. doi:10.3389/fimmu.2022.952040
41. Wu M, Guo H, Liu L, Liu Y, Xie L. Size-dependent cellular uptake and localization profiles of silver nanoparticles. *Int J Nanomed*. 2019;14:4247–4259. doi:10.2147/IJN.S201107
42. Azad GK, Tomar RS. Ebselen, a promising antioxidant drug: mechanisms of action and targets of biological pathways. *Mol Biol Rep*. 2014;41 (8):4865–4879. doi:10.1007/s11033-014-3417-x
43. Yang Y, Guo L, Wang Z, et al. Targeted silver nanoparticles for rheumatoid arthritis therapy via macrophage apoptosis and Re-polarization. *Biomaterials*. 2021;264:120390. doi:10.1016/j.biomaterials.2020.120390
44. Farkas J, Christian P, Gallego-Urrea JA, et al. Uptake and effects of manufactured silver nanoparticles in rainbow trout (Oncorhynchus mykiss) gill cells. *Aquat Toxicol*. 2011;101(1):117–125. doi:10.1016/j.aquatox.2010.09.010
45. Bolduc JA, Collins JA, Loeser RF. Reactive oxygen species, aging and articular cartilage homeostasis. *Free Radic Biol Med*. 2019;132:73–82. doi:10.1016/j.freeradbiomed.2018.08.038
46. Bi CL, Wang H, Wang YJ, et al. Selenium inhibits Staphylococcus aureus-induced inflammation by suppressing the activation of the NF-kappaB and MAPK signalling pathways in RAW264.7 macrophages. *Eur J Pharmacol*. 2016;780:159–165. doi:10.1016/j.ejphar.2016.03.044
47. Cekici A, Kantarci A, Hasturk H, Van Dyke TE. Inflammatory and immune pathways in the pathogenesis of periodontal disease. *Periodontol 2000*. 2014;64(1):57–80. doi:10.1111/prd.12002